Second Harmonic Injection With Model Predictive Control: Attenuation of DC-Link Pulsations in Single-Phase Inverters

Liwei Zhou, *Member, IEEE*, Noah Silverman, *Graduate Student Member, IEEE*, and Matthias Preindl, *Senior Member, IEEE*

***Abstract*—A model predictive control-based second harmonic injection (MPC-SHI) method is proposed in this article to attenuate the dc side second pulsation for the single-phase inverter. The directly calculated second harmonic injection (SHI) component is configured as the tracking reference and regulated by the model predictive control (MPC) with improved dynamic performance. The combination of MPC and SHI enhances the transient behavior with less response time and oscillation. Compared with the conventional methods, no extra notch filter or band-pass filters are needed to deal with the second order harmonics in the control process. The control bandwidth is increased with more tuning flexibility and better dynamic performance. No extra passive or active components are needed to attenuate the dc side second pulsation. The cost is largely saved accordingly. The experimental results have validated the proposed method.**

***Index Terms*—*LCL* filter, model predictive control, power decoupling, second harmonic injection, second order pulsation, single-phase inverter.**

I. Introduction

SINGLE-PHASE grid-connected inverters have been widely applied in the renewable energy conversion systems and microgrid systems [1], [2], [3]. Solar energy, battery storage systems and other dc energy resources typically need the single-phase inverters to deliver low power energy conversion to be connected with the ac grid. With the development of clean energy and the target of net-zero emission, the microinverters are attracting more research focus since the inverter-based distributed energy resources are the major components to form a microgrid renewable system [4], [5]. Single-phase inverter is one of the crucial types of microinverter for the energy conversion system [6], [7]. The performance of the single-phase inverter largely determines the popularization of distributed renewable energy resources. Some key issues have been studied to improve the single-phase inverter including the second order pulsation, control dynamic performance, and leakage current [8], [9], [10].

First, one of the biggest issues for designing a single-phase inverter is the second-order pulsation on the dc side. The main function of the single-phase inverter is to converting the power from dc to ac side. However, due to the unbalanced ac and dc power, there exists a second-order ac pulsation on the dc side. This pulsation is stored and released through the dc sources. Otherwise, a huge dc capacitor is required to damp this unbalanced power by charging and discharging the ac pulsation. Several techniques have been studied to attenuate this second-order pulsation including the passive and active power decoupling methods. For the passive method, the main idea is to leverage the magnetic components of inductors and capacitors for the dc side second pulsation reduction [6], [11], [12]. Either split dc capacitors or *LC* circuits can be inserted between the dc and ac for the power decoupling. For the active method, extra switches are required to form the auxiliary circuits for the second pulsation attenuation [4], [13], [14], [15], [16], [17]. Among the conventional power decoupling methods for the single-phase inverters, most of the control strategies are applying the proportional integral derivative (PID), proportional resonant (PR), or notch filter algorithms [4], [10], [18], [19]. The targeted even order of the fundamental grid frequency harmonics can be mitigated accordingly. However, the transient performance has been sacrificed due to the extra damping controllers. The lack of improved dynamic performance for the power converter can cause several issues including: 1) high overshoot during transient which could cause the overcurrent/overvoltage circuit damage; 2) long rise time during transient which could delay the reference tracking and worsen the control accuracy especially for the applications that require high-frequency reference variations and fast response.

Second, from the control perspective of single-phase inverters, PID has been the most widely utilized technology in the industry due to the implementing simplicity and tuning flexibility. However, the aforementioned second order pulsation on the dc side can affect the ac side power quality through the dq reference frame control loop. This is resulted from the cascaded control loop including the former stage of dc bus voltage controller followed by the latter stage of d component ac current controller. Furthermore, the affected d component

Received 10 June 2024; revised 20 September 2024 and 30 November 2024; accepted 28 December 2024. Date of publication 2 January 2025; date of current version 26 February 2025. Recommended for publication by Associate Editor S. Golestan. *(Corresponding author: Matthias Preindl.)*

Liwei Zhou is with the Department of Electrical Engineering, University of Texas at Arlington, Arlington, Texas 76010 USA (e-mail: liwei.zhou@uta.edu).

Noah Silverman and Matthias Preindl are with the Department of Electrical Engineering, Columbia University, New York City, New York 10027 USA (e-mail: nhs2134@columbia.edu; mp3501@columbia.edu).

Color versions of one or more figures in this article are available at https://doi.org/10.1109/TPEL.2024.3525390.

Digital Object Identifier 10.1109/TPEL.2024.3525390

output current will be transformed into abc reference frame as the duty cycles for carrier-based modulation. This type of second order pulsation will worsen the corresponding output ac current. Thus, the output power quality on the ac side will be deteriorated. Yao et al. [20] compared the ac output current waveforms with and without the second pulsation power decoupling method. It showed that the power decoupling can improve the current distortion by mitigating the high order harmonics. Higher value of the filters could be added to attenuate different orders of the harmonics. However, extra filters can worsen the control performance with lower bandwidth. Tang et al. [12] showed the magnitude response of the impedance ratio with the ac side inductance and CM inductance to be changed from 0.2 to 1 mH. With the increasing of the filter value, the bandwidth has been decreased accordingly. The mechanism of notch filter is to filter out the specific targeted range of frequency and pass the other frequencies without being changed. The band-stop range of the notch filter can be adjusted by the parameter. However, the notch filter can affect the adjacent frequencies at the edges of the band-stop range with distorted amplitude and phase. Besides the notch filter PR-based method, other control strategies have also been studied to deal with the second pulsation including the PR, repetitive control and model predictive control (MPC). Tang et al. [12] developed a PR controller to mitigate the influence of second harmonics on the control loop. Zeng et al. [21] designed a repetitive controller to mitigate the second harmonics induced by the oscillation on the dc bus. Gautam and Fulwani [22] proposed a sliding mode control to reduce the single-phase inverter dc ripple for the dc microgrid applications by leveraging the output impedance shaping of the dc source. Xu et al. [23] developed another energy-based control strategy to deal with the second-order pulsation for the buck–boost type of single-phase inverter. The active damping control has been studied to reduce the dc oscillation at the resonant frequency. Among the above-mentioned control methods, MPC has been recognized as one of the promising solutions [24], [25], [26], [27]. MPC has the advantages of better dynamic performance with less rise time, overshoot, and more robust operation [28], [29], [30]. There are limited studies on leveraging the MPC to solve the second pulsation issue for the single-phase inverters.

The contributions of this article can be summarized as follows.

1) A combined MPC-SHI method is proposed to largely reduce the second pulsation issue for single-phase inverter;
2) The dynamic performance and control bandwidth of the SHI are improved with MPC regulation.
3) The THD and leakage current of the designed method are both low with the zero-sequence MPC-SHI control method;
4) No extra passive or active components are needed to achieve the second pulsation attenuation. The cost is largely reduced.

II. Second-Order Pulsation in Single-Phase Inverter

A. Second Order Pulsation Issue

In a single-phase inverter system as shown in Fig. 1, the ac side output power $P_{\mathrm{AC,grid}}$ can be expressed as

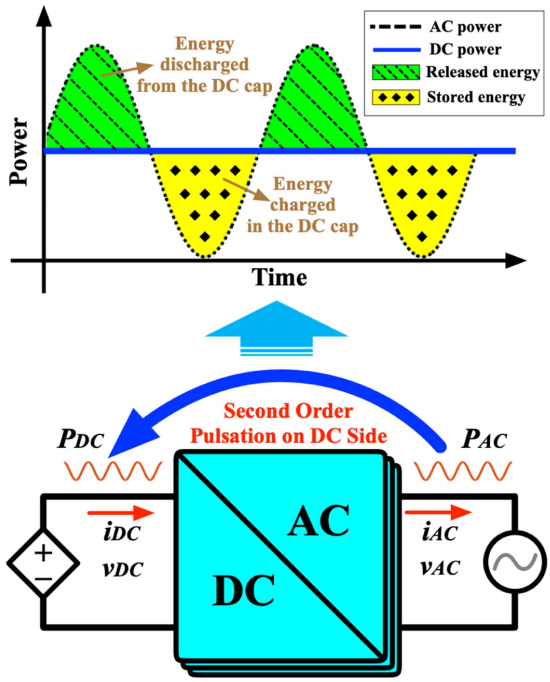

Fig. 1. General single-phase inverter topology and the existing second pulsation issue on the dc side.

$$P_{\mathrm{AC,grid}} = V_{\mathrm{AC,grid}} I_{\mathrm{AC,grid}} \frac{1-\cos(2\omega t)}{2} \tag{1}$$

where $v_{\mathrm{AC,grid}}(t)$, $i_{\mathrm{AC,grid}}(t)$, $V_{\mathrm{AC,grid}}$, and $I_{\mathrm{AC,grid}}$ are the instantaneous values and amplitudes of the ac side output voltage/current. However, the dc side power $P_{\mathrm{DC,bus}}$ can be demonstrated as

$$P_{\mathrm{DC,bus}} = v_{\mathrm{DC,bus}}(t) i_{\mathrm{DC,bus}}(t) \tag{2}$$

where $v_{\mathrm{DC,bus}}(t)$ and $i_{\mathrm{DC,bus}}(t)$ are the instantaneous values of dc side voltage/current.

Due to the balanced power between the dc input and ac output side, the input dc side current can be further derived as

$$i_{\mathrm{DC,bus}}(t) = V_{\mathrm{AC,grid}} I_{\mathrm{AC,grid}} \frac{1-\cos(2\omega t)}{2 v_{\mathrm{DC,bus}}(t)}. \tag{3}$$

Thus, either the dc side is connected to constant voltage/current sources or designed as a dc bus to be linked with other energy stages, the dc side will be inevitably oscillating at twice of the fundamental grid frequency due to the processes of storing and releasing the imbalanced energy from the dc capacitor as shown in Fig. 1. This second-order fluctuation could worsen the power quality of the single-phase inverter, especially when the value of the dc capacitance is not high enough to mitigate the charge and discharge of the unbalanced energy between the dc and ac sides. Some typical power quality issues, such as the output side voltage/current waveforms distortion, saturation and unstable conditions, may happen and even result in power failure.

B. State-of-the-Art Solutions

The conventional second pulsation power decoupling technologies can be divided into passive and active strategies. As

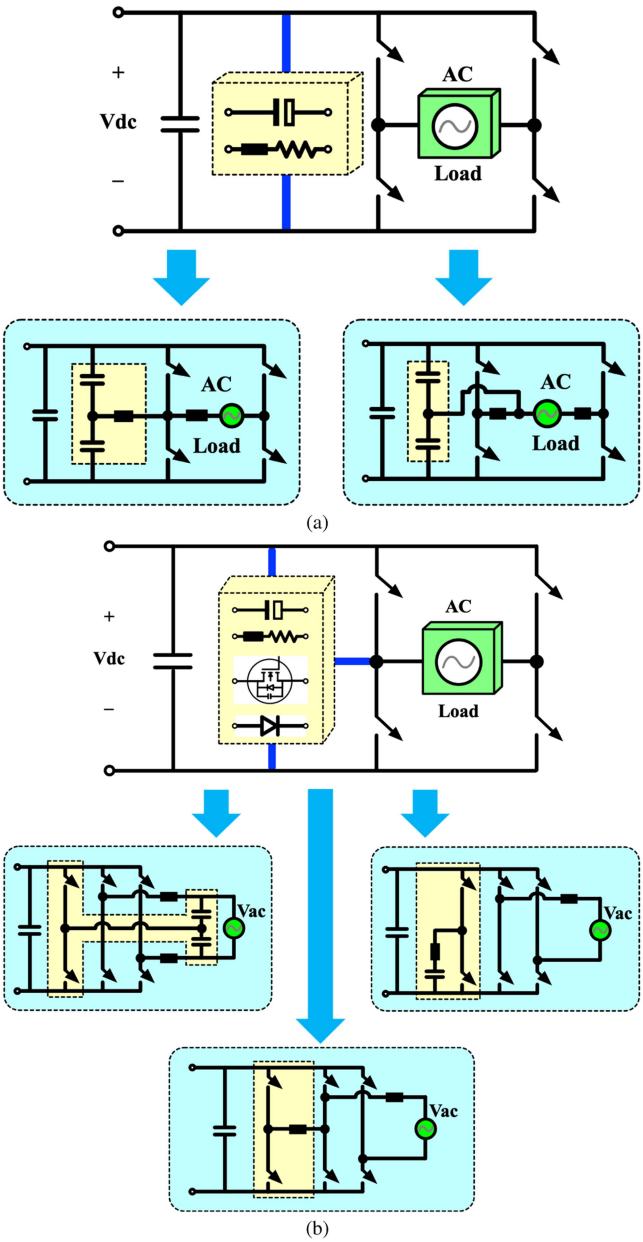

Fig. 2. (a) Passive [20], [31], [32], [33], [34], [35] and (b) active [13], [15], [16], [36], [37], [38], [39], [40] second pulsation power decoupling methods for single-phase grid-tied inverters including two passive power decoupling single-phase inverter topologies in [20] and [31] and three active power decoupling single-phase inverter topologies in [13], [15], and [16].

shown in Fig. 2(a), the passive strategies apply extra power capacitors or inductors to attenuate the second-order pulsation of twice grid frequency [32], [33], [34], [35]. Two separate capacitors could be inserted on the dc bus terminal side. The middle point of the dc bus can be linked to the output point of the switching phase module via an inductor or directly linked to the ac side. Typically, this type of method needs a high value of capacitance to store and release the fluctuating ac power. However, this type of technology normally costs more. In addition, another type of method is in an active way to further attenuate the second order pulsation with extra switching circuit as shown in Fig. 2(b) [36], [37], [38], [39], [40]. Instead of purely

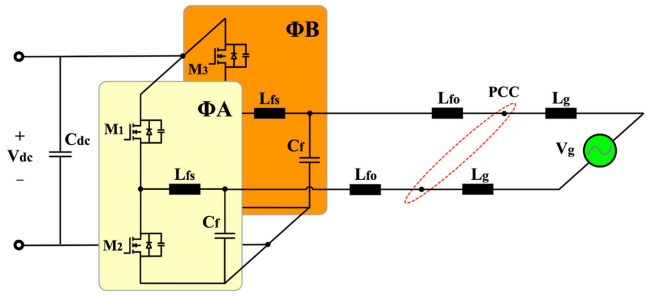

Fig. 3. Circuit topology of the single-phase inverter for the implementation of the proposed MPC-regulated second harmonic injection method [36], [37], [38], [39], [40].

utilizing the passive components, specially designed switch circuit can be leveraged to actively control and mitigate the second order pulsation. One of the fundamental strategies is by inserting an extra switching phase module between the ac and dc sides. The additional switching phase module could be linked to either the ac side through separate power capacitors, dc negative point via a series-connected inductor and capacitor or another switching phase module output terminal via an inductor. The merit of the active strategy is that no high value of capacitance is required to mitigate the second order pulsation. However, the corresponding specially designed power decoupling control strategies are required to deal with the second order pulsation between the ac and dc sides. The corresponding control algorithms are normally linked with the design of notch filter, band-pass filters, or PR controllers for the purpose of managing the even order harmonics of the grid frequency. However, this codesign and consideration are tradeoff and will sacrifice the single-phase inverter power operation performance with lower control bandwidth. Also, extra switching and magnetic circuits result in more cost and complexity. The operation reliability is another concern that needs to be addressed when designing and operating the extra circuits.

III. Proposed MPC-Based SHI Method

A. Methodology

1) Control Structure: The proposed control algorithms are implemented in a full bridge single-phase inverter as shown in Fig. 3, where the ac output capacitors are connected to the dc bus terminals. The proposed control structure for the single-phase inverter has been shown in Fig. 4 including the $dq0$ reference frame control to be cascaded with the per phase MPC control.

Specifically, for the $dq0$ reference frame control, first, the dc voltage is cascaded with the d component of the grid current $i_{g,d}$ controller to provide the d component reference for the output capacitor voltage MPC control. Second, the reactive power Q controller is cascaded with the q component of the grid current $i_{g,q}$ controller to provide the q component reference for the output capacitor voltage MPC control. Third, the zero sequence control is responsible for the common mode voltage stabilization and second harmonic injection derivation to be configured for the zero sequence reference of the MPC control.

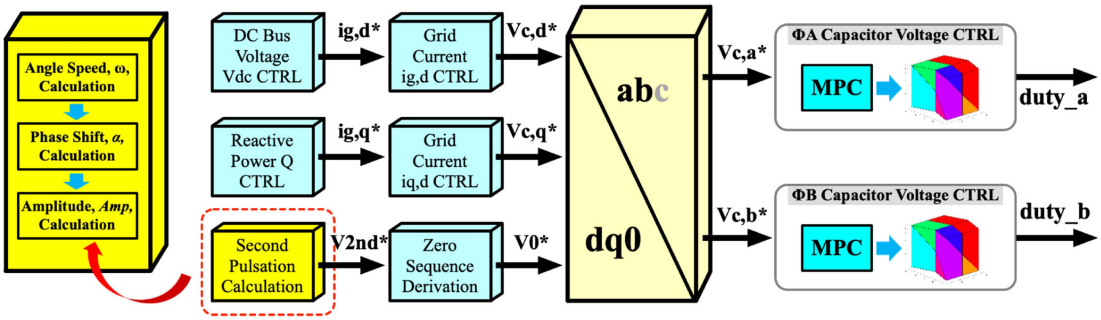

Fig. 4. Control diagram of the single-phase inverter with the proposed MPC-regulated second harmonic injection method.

The output capacitor voltage references $V^*_{c,dq0}$ are then transferred from $dq0$ reference frame to the ab reference frame for the per phase output capacitor voltage MPC control. The implementation of the MPC is to receive the sampled ac inductor current $i_{L,ab}$, lower capacitor voltage $v_{Cf,ab}$, grid current $i_{g,ab}$, from ADC and lower capacitor voltage reference $v^*_{c,ab}$ from the output of the upper level cascaded grid current controller/zero sequence derivation. The MPC is executed explicitly with a preconfigured piecewise affine function to generate the desired duty cycle for the per phase switching modulation.

For the digital execution of MPC, the state space equations can be configured as

$$i_L(k+1) = i_L(k) - \frac{T_s}{L_{fs}}u_c(k) + \frac{v_{DC}T_s}{L_{fs}}d(k)$$
$$v_{Cf}(k+1) = \frac{T_s}{C_f}i_L(k) + v_{Cf}(k) - \frac{T_s}{C_f}i_g(k). \quad (4)$$

The standardized matrix format can be expressed as

$$X_{k+1} = AX_k + Bu_k + Ee_k \quad (5)$$

where $A = [1, -T_s/L_{fs}; T_s/C_f, 1]$, $B = [T_s/L_{fs}; 0]$, $E = [0; -T_s/C_f]$, $X_k = [i_L(k); v_{Cf}(k)]$, $u_k = [v_{DC}d(k)]$ and $e_k = [i_g k]$.

The cost function is composed of two items

$$\min \sum_{k=0}^{N_c} \tilde{X}_k^T Q \tilde{X}_k + \sum_{k=0}^{N_p-1} \triangle u_k^T R \triangle u_k \quad (6)$$

where $\tilde{X}_k = [i^*_L(k) - i_L(k); v^*_{Cf}(k) - v_{Cf}(k)]$, $\triangle u_k = u_k - u_{k-1}$ and Q, R represent the weighting matrices for the tracking error and input variable terms in the cost function. Typically, the weighting of $v^*_{Cf}(k) - v_{Cf}(k)$ in $\tilde{X}_k$ is configured to be 100–500 times larger than other terms. The reasons to configure $\tilde{X}_k$ with such range can be summarized as: 1) the main purpose of MPC is to track the output capacitor voltage. More weighting factor on $\tilde{X}_k$ aims to achieve a more accurate capacitor voltage tracking performance; 2) The other term of $\triangle u_k$ is mainly focused on the mitigation of the adjacent duty cycles variation which is less significant than the output capacitor voltage tracking. The typical weighting between these two terms is configured to be larger than 100 times. For the zero sequence component of the output capacitor voltage MPC reference $v^*_{Cf,0}$, in Fig. 5, it is composed of two terms, zero sequence offset voltage reference

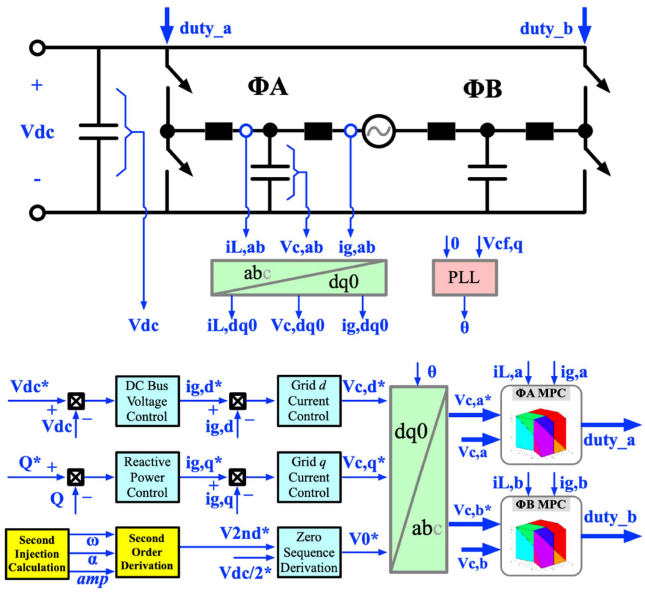

Fig. 5. Detailed control implementation of the proposed MPC-regulated second harmonic injection method.

of half dc bus averaged voltage $v_{DC}/2$, and the calculated second harmonic injection v_{2nd}

$$v^*_{Cf,0} = v_{DC}/2 + v_{2nd}. \quad (7)$$

The per phase output capacitor voltage MPC controllers regulate and track the desired second harmonic injection v_{2nd}, with more stable operation and higher bandwidth to achieve the second-order power decoupling. No extra notch filter or resonant controller is needed to damp the second pulsation. Also, the MPC improves the dynamic performance with higher control bandwidth, faster response time, and less transient oscillation. The detailed control diagram has been shown in Fig. 5.

2) Second Harmonic Injection Derivation: For the MPC-regulated second harmonic injection derivation in the zero sequence control branch of control structure, the proposed method is leveraging the direct calculation based on the balanced charging/discharging between the ac/dc capacitors. No extra notch filter or band-pass filter is needed to filter out or extract the second harmonic component. The control bandwidth is largely improved due to the combination of direct calculation and MPC

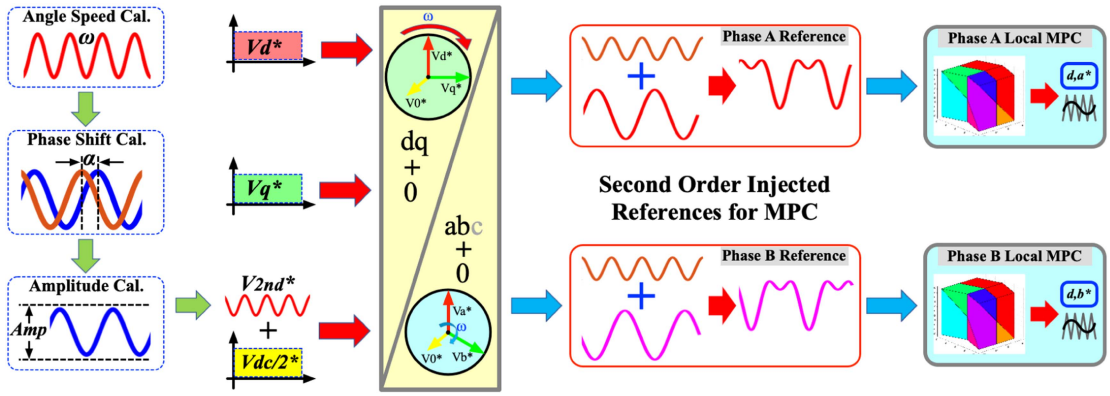

Fig. 6. Detailed waveforms and principle of the proposed MPC-regulated second harmonic injection method.

regulation. The core methodology is to transfer the second pulsation from the dc side capacitor C_{dc} to the output lower capacitors $C_{f,lo}$ for the purpose of stabilizing the dc side second pulsation. Three steps are designed to derive the desired second harmonic injection as shown in Fig. 6.

First, the angle speed of the second harmonic injection is derived as twice of the grid line frequency $2\omega_0$, according to the calculation in (3).

Second, the phase shift α of the second harmonic injection is calculated based on the angular difference between the vectors of $i^*_{g,d}$ and $i^*_{g,q}$ by following

$$\alpha = \arctan \frac{i^*_{g,d}}{i^*_{g,q}}. \tag{8}$$

Third, the amplitude of the second harmonic injection V_{amp} is derived based on the balanced charging/discharging between the ac/dc capacitors C_{dc} and $C_{f,lo}$. To balance the second pulsation energy between the ac/dc capacitors, the voltage ripples should satisfy the following charging/discharging equation:

$$\frac{1}{2}C_{dc}\Delta v^2_{DC} = 2\left(\frac{1}{2}C_{f,lo}\Delta v^2_{Cf}\right). \tag{9}$$

The voltage ripple on the dc bus capacitor Δv_{DC} can be expressed as

$$\Delta v_{DC} = \frac{V_{AC,grid}I_{AC,grid}}{2\omega_0 C_{dc} v_{DC,avg}} \tag{10}$$

where $v_{DC,avg}$ and ω_0 are the averaged dc bus voltage and grid line frequency, respectively. Then, the desired amplitude of the second harmonic injection on the ac output capacitor voltage can be derived from (9) and (10) as

$$V_{amp} = \frac{V_{AC,grid}I_{AC,grid}}{\omega_0 v_{DC,avg}\sqrt{8C_{dc}C_{f,lo}}}. \tag{11}$$

Finally, the desired second harmonic injection can be expressed as

$$v_{2nd} = V_{amp}\cos(2\omega_0 t + \alpha + \epsilon) \tag{12}$$

and leveraged for the per phase MPC control and regulation. The term of ϵ represents the phase shift constant by considering the initial difference of sine or cosine functions.

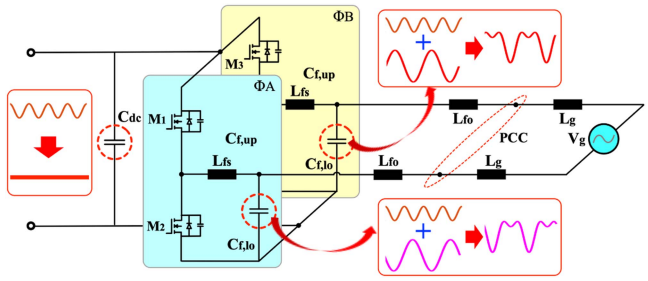

Fig. 7. Mechanism of the proposed MPC-regulated second harmonic injection method.

The injected second harmonic component is fluctuating at two times of the grid frequency (60 Hz). Compared with the switching frequency of hundreds of kilohertz, the fluctuating rate of the second harmonic component is low. Since the value of common mode current i_{cm} is mainly dependent on the change rate of the common mode voltage v_{cm} and parasitic capacitance C_p, with a relation of $i_{cm} = C_p \mathrm{d}v_{cm}/\mathrm{d}t$, the leakage current and common mode voltage/current performance will not be affected or worsened by the second harmonic injection which has also been validated in the results section with a low leakage current of less than 10 mA.

For a more intuitive expression of the MPC-SHI implementation, the operating mechanism of the injected second harmonics and the corresponding physical components are shown in Fig. 7.

B. Control Performance Analysis and Comparison

For the purpose to showcase the advantages of better control performance and second pulsation mitigation of the proposed MPC-based second harmonic injection (MPC-SHI) method, the detailed analysis between the developed strategy and the traditional methods are further demonstrated in this section.

The control diagrams comparison of the proposed MPC-SHI and the conventional SHI have been shown in Figs. 5 and 8. The conventional strategy to mitigate the second order fluctuation is usually configuring a band-pass or notch filter in the

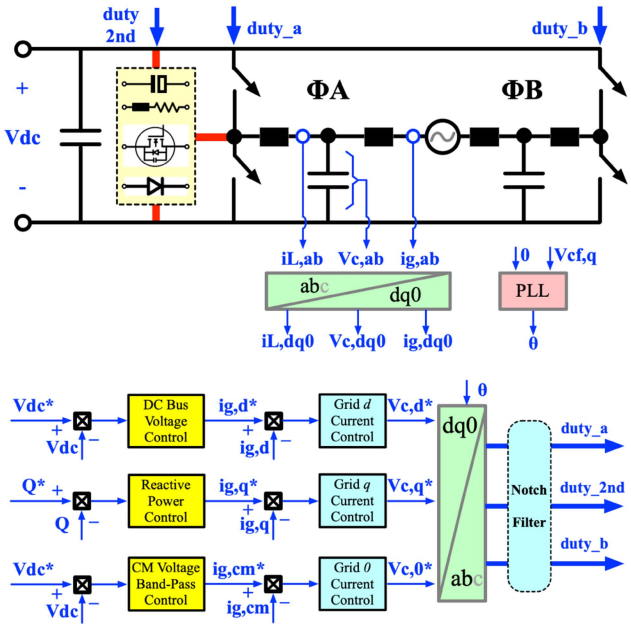

Fig. 8. Control implementation of notch filter PR control of second pulsation power decoupling method.

dc control branch to reduce the influence of second fluctuation on the d components of voltage/current. In addition, in the 0 sequence branch of the traditional method, the expected second-order harmonic components are usually derived via the specially designed band-pass filters for the purpose of second harmonic injection as addressed in the yellow areas of Fig. 8. However, these band-pass or notch filters and controllers can worsen the regular power control with lower bandwidth. On the other hand, the developed MPC-SHI in this article combines the directly calculated second harmonic value into the MPC control reference. Therefore, no additional band-pass or notch filters are needed to be inserted in the control loop. Due to the elimination of extra filters, the bandwidth for power regulation and control can be improved with better transient performance (faster rise time, less overshoot).

1) Notch Filter PR Control: For the notch filter PR control or active methods in Fig. 8, since the dq branches of the dc bus and reactive power controllers can both be affected by the second pulsation, the twice grid line frequency $2\omega_0$, notch filter is typically added to keep the corresponding second harmonic components from worsening the output voltage/current waveforms quality. Also, in the 0 sequence branch of the common mode component controllers, the specially designed band-pass filters are typically added to deal with the second or fourth order harmonics, $2\omega_0$ and $4\omega_0$.

2) Proposed MPC-SHI Control: For the proposed MPC-SHI control method in Fig. 5, since the second pulsation on the dc bus can be largely attenuated through MPC regulation, the dq branches of the dc bus and reactive power controllers will not be influenced by the second pulsation. Thus, compared with the traditional PI method, no second order notch filter on dq or band-pass filter on zero sequence control branches is needed to improve the output power quality. The control bandwidth and dynamic performance can both be improved, accordingly.

TABLE I
COMPARISON OF OPTIMAL POWER CONVERTER CONTROL METHODS

	LQR	LQG	MPC
Applicable system	Linear	Linear	(Non)Linear
Anti-noise Capability	No	Yes	Yes
Cost function	Quadratic	Quadratic	Custom
Constraints Handling	No	No	Yes
Predictive Capability	No	No	Yes

3) Comparison of MPC and LQR/LQG for Inverter Control: For the optimal control implementation besides the MPC, the linear quadratic regulator (LQR) and linear quadratic Gaussian (LQG) are two other methods. LQR is an optimal control for linear systems, which requires a linear system model in the state-space form to minimize a quadratic cost function that penalizes deviations in state variables and control inputs. LQG combines LQR with a state estimator (Kalman Filter) for systems with uncertainty to optimize control performance in the presence of process and measurement noise. The detailed comparison has been shown in Table I. First, MPC can handle constraints which is not applicable for LQR/LQG. Power converters typically operate with strict voltage, current, and switching constraints to ensure safe operation, efficiency, and to avoid damage. Second, MPC can account for the nonlinear behavior of power converters by incorporating the actual nonlinear system model and using linear approximations over a prediction horizon. Third, MPC can predict future behavior of the system over a finite horizon based on a dynamic model. This is particularly useful in power converters for controlling fast high switching frequency dynamics with better transient performance. For the implementation of the proposed MPC in single-phase inverter, the control parameters are 500 for the weighting factor, Q/R in (6), 2 for the moving horizon, ± 500 V for the ac and dc voltage constraints, ± 50 A for the ac current constraints.

IV. MERITS VALIDATION AND COMPARISON

The developed MPC-SHI has been validated experimentally and compared with the conventional methods to show the merits in the following four aspects:

1) steady-state performance of dc side second pulsation attenuation;
2) improvement on the transient performance and robustness due to the MPC regulation;
3) mitigation of the leakage current and THD on the ac output side;
4) reduction on the passive and active component cost.

A 1-kW single-phase inverter test bench is connected to the grid simulator for the experimental validation. The switching frequency is configured as 80 kHz. The filter parameters are designed as 45 μH for switch side inductance, 24 μF for ac side capacitance, and 144 μF for dc side capacitance. The Cree SiC MOSFET of C3M0021120K is leveraged for the power switches. The TI DSP of TMS320F28379D is configured as the microcontroller.

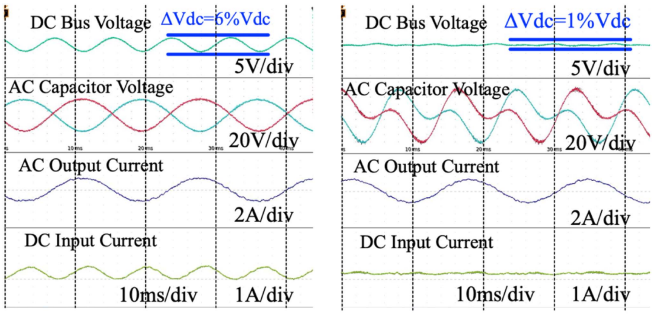

Fig. 9. Steady-state performance of DC bus voltage, AC capacitor voltage, AC output current, AC inductor current, and DC input current (a) without and (b) with the proposed MPC-based second harmonic injection method for the single-phase inverter connected to a DC power supply.

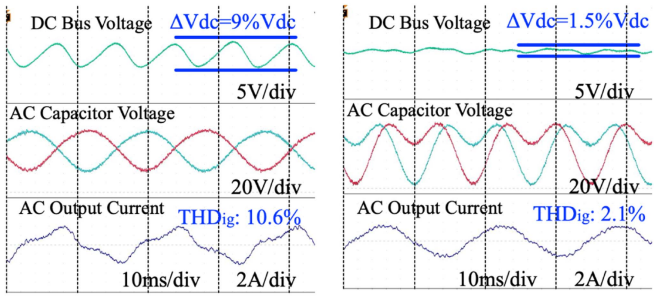

Fig. 10. Steady-state performance of DC bus voltage, AC capacitor voltage, AC output current, and AC inductor current (a) without and (b) with the proposed MPC-based second harmonic injection method for the single-phase inverter with a floating DC bus.

The tradeoff between the switching losses and predictive control response performance with different switching frequencies has been discussed as follows. A higher control frequency is typically affiliated with a relatively high switching frequency to achieve a better control response for the predictive control. However, the extra switching losses will be induced due to the high switching frequency. The setup in this article configures a 20-kHz control frequency, 80-kHz switching frequency, and 40-kHz sampling frequency. Since the execution of the MPC algorithms accounts for around 4–6 μs in each control interrupt, it is challenging to configure a high control frequency to improve the control response. For a typical TI DSP of TMS320F28379D, the computation capability can handle most of the algorithm execution for the power switches at 20-kHz control frequency with 50 μs in each interrupt. Thus, the switching frequency can be configured as multiple integer times of the control frequency, such as 40, 60, 80, 100 kHz, etc. The selection of the switching frequency is then based on the inductor/capacitor values and output current/voltage ripples. We selected 80 kHz to be combined with 45 μH for switch side inductance, 24 μF for ac side capacitance.

TABLE II
STEADY-STATE PERFORMANCE COMPARISON

	MPC-based SHI	PI-based SHI	Passive circuit	Active circuit
Reference tracking error	2%	5%	4.5%	3.8%
AC output current THD	1.5%	5.6%	4.3%	3.2%
DC current oscillation	5.2%	12.5%	8.4%	7.6%

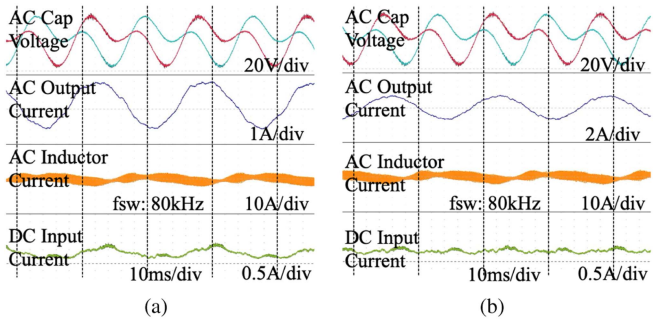

Fig. 11. Steady-state comparison of AC capacitor voltage, AC output current, AC inductor current, and DC current between the (a) notch filter PR-based method and the (b) proposed MPC-based second harmonic injection method.

A. *Steady-State Performance of Second Pulsation Attenuation*

For the dc side second pulsation attenuation, Fig. 9 shows the steady-state performance of dc bus voltage, ac capacitor voltage, ac output current, ac inductor current, and dc input current without and with the MPC-SHI method for the single-phase inverter by connecting the dc bus to a dc voltage source power supply. Fig. 10 demonstrates the steady-state performance of dc bus voltage, ac capacitor voltage, ac output current, and ac inductor current without and with the MPC-SHI method for the single-phase inverter by floating the dc bus. It can be seen that the dc second pulsation voltage ripple Δv_{DC} has been reduced by six times from 6% to 1% and 9% to 1.5%, respectively, which are better than the conventional methods of 3.2 times in [36] and 1.8 times in [40].

The steady-state performance of the proposed MPC-based method and the notch filter PR-based method has been compared in the aspects of tracking accuracy, ac output power quality, and dc oscillation in Table II. The corresponding waveforms have also been demonstrated in Fig. 11. The MPC method improved the tracking accuracy, output THD, and dc oscillation by 2.5, 3.7, and 2.4 times, respectively. The amplitude of the second, fourth current harmonics are less than 0.1%, which are 1.2–2 times smaller than the other control strategies in Table II.

In addition, the comparison with other second pulsation mitigation methods has also been shown in Table II including the passive circuit method and active circuit method [13], [20]. Different from the pure control methods of either MPC-based or PI-based strategies, the passive and active circuit methods typically combined the extra passive/active components with the corresponding PI or PR control strategies to deal with the second pulsation. Thus, the corresponding performances of output power quality and dc oscillation are better than the pure PI-based control method at the cost of extra hardware components and power losses.

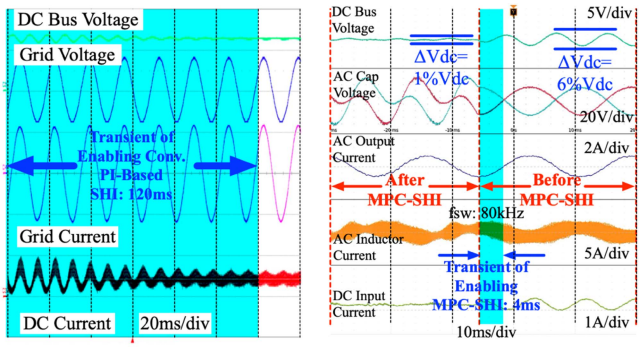

Fig. 12. Transient performance comparison of DC bus voltage, AC capacitor voltage, AC output current, AC inductor current and DC current by enabling the (a) notch filter PR-based SHI and the (b) proposed MPC-SHI method.

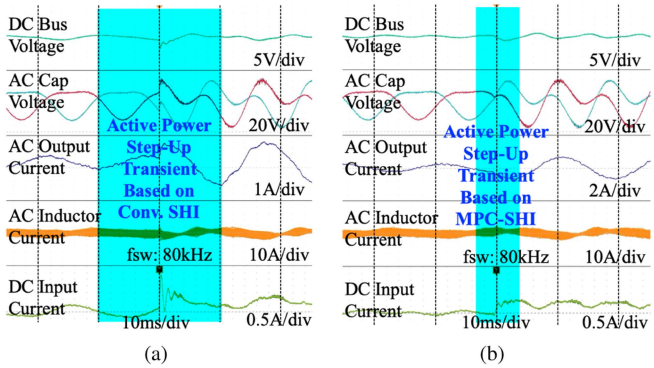

Fig. 13. Transient performance comparison of the (a) notch filter PR-based SHI and the (b) MPC-SHI method with an active power reference step-up.

The computation burden is another essential topic that is discussed as follow for different control strategies. The developed MPC algorithm is efficient in computation and compact in memory size. These merits enable the use of the DSP to implement the MPC algorithm in the power converter applications. An explicit method is leveraged to derive the control algorithm by generating the piecewise affine control functions without implementing the time-consuming online optimization process. The computation burden is saved correspondingly. The memory size is less than 5 KB with an execution time of less than 4 μs. This is less than the typical finite-control-set (FCS) MPC of 18 μs, discrete-space-vector-modulation (DSVM) MPC of 64.8 μs in [41], and another DSVM MPC method of 26.6 μs in [42].

B. Improved Transient Performance and More Robust Behavior With MPC Regulation

For the transient performance, since MPC-based SHI improves the control bandwidth with more flexibility to enhance the control gain, the rise time, and overshoot are both significantly reduced compared with the notch filter PR-based control method. Fig. 12(a) shows the transient performance of dc bus voltage, ac grid voltage, ac output current, and dc input current by enabling the notch filter PR-based second harmonic injection method of [12]. Fig. 12(b) demonstrates the transient periods of dc bus voltage, ac capacitor voltage, ac output current, and ac inductor current by enabling the proposed MPC-based second harmonic injection method. It can be seen the transient period of the notch filter PR method lasts for 120 ms. The proposed MPC-SHI can largely shorten the transient period by 40 times to only 3 ms without oscillation. In addition, Fig. 13(a) demonstrates the transient performance comparison of the notch filter PR-based SHI and the proposed MPC-SHI methods with the active power reference step-up. It can be shown that the transient waveforms of the notch filter PR-based method are oscillating with much bigger overshoot than the MPC-SHI, especially for the dc side current.

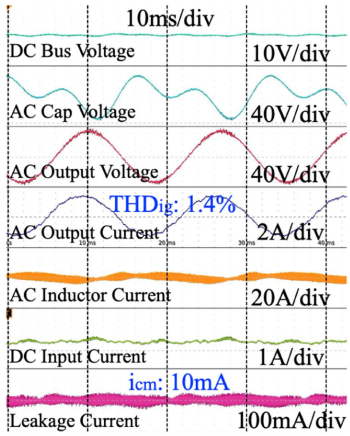

Fig. 14. Output voltage/current power quality and the leakage current for the proposed MPC-SHI control method.

C. Low Leakage Current and THD in the AC Output Side

The proposed MPC-based control method can mitigate both the dc side second pulsation and ac side leakage current without distorted power quality since the injected second-order harmonics are managed to merely circulate within the switch side LC filter. Thus, the ac output side current quality can be maintained under low THD. Fig. 14 shows the grid voltage/current and leakage current waveforms. The THD of grid voltage/current are kept below 2.5% and the leakage current is within 10 mA. The comparison of the THD with and without the MPC-SHI has been demonstrated in Fig. 10(b) where the power quality of the grid side output current THD has been reduced from 10.6% to 2.1% due to the proposed SHI method.

D. Less Passive and Active Component Cost

From cost perspective, the proposed control strategy enables a reduction on hardware cost since the proposed method is merely utilizing the control algorithm to mitigate the second oscillation without inducing extra physical components. In addition, from control perspective, compared with the notch filter PR-based power decoupling control methods in [12], [36], [37], [38], [39], [40], and [43], the proposed MPC-SHI improves the dynamic

TABLE III
COST AND PERFORMANCE COMPARISON

	Active Components	Passive Components
MPC-SHI	4 switches	2 ind., 3 cap.
[12]	4 switches	2 ind., 4 cap.
[36]	6 switches	3 ind., 2 cap.
[37]	6 switches	2 ind., 2 cap.
[38]	4 switches	3 ind., 3 cap., 2 dio.
[39]	6 switches	3 ind., 3 cap., 3 dio.
[40]	8 switches	1 ind., 2 cap.
[43]	4 switches	2 ind., 2 cap.

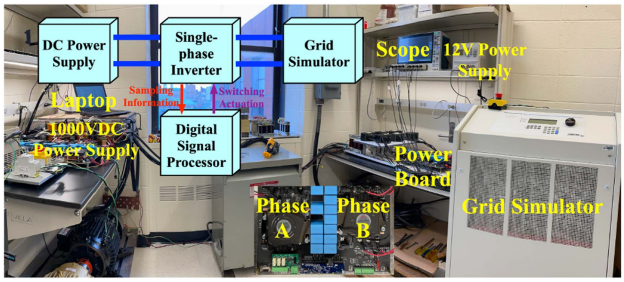

Fig. 15. Setup of the testbench.

performance with less rise time and overshoot. A summary table of the cost performance comparison among different studies has been demonstrated in Table III. It can be shown that the proposed method achieves less cost on the switches/diodes, inductors, and capacitors. The setup for the implementation of the proposed method has been shown in Fig. 15. For the conventional second pulsation control studies, authors in [12], [37], [38], and [40] developed the PR-based control, while [36], [39], and [43] leveraged the PI-based control methods. Typically, PI control is ideal for dc signal control and cannot effectively handle the second oscillating ac signals with zero steady-state error. However, PR control includes a resonant term to achieve zero steady-state error when tracking ac signals, making it more proper for the second pulsation control and management. Also, PR has better dynamic performance than PI especially in tracking the ac signals. However, the PR typically requires careful design to place the resonant term at the correct frequency which is regarded as a more complex system. The detailed control performance of the conventional PI/PR studies can be summarized as follows. Tang et al. [12] has a transient period of 100 ms at a 360 W load change with a dc current overshoot of 40%. Hu et al. [36] performed a transient period of 180 ms at a 90% load change with a dc voltage overshoot of 8.3%. Fantino et al. [37] has 20 ms transient period at a 800 W load change with a dc current overshoot of 50%. The settling time for [38] is 200 ms for the load to be changed from 72 to 36 Ω. Paul et al. [39] demonstrated a 220 ms transient period for grid current change. Heydari et al. [40] achieved 25 ms transient period by dropping the output power from 1000 to 640 W with a dc voltage overshoot of 15%. Eren et al. [43] performed a 23 ms transient period at a 50% rated power step change with a dc voltage overshoot of 12.5%.

V. CONCLUSION

This article proposes an MPC-regulated second harmonic injection method for the single-phase inverter to attenuate the dc side second pulsation. The proposed method integrates the calculated second harmonic injection with the MPC to improve the dynamic performance. Since the directly calculated second harmonic component is regulated by the MPC controller before injecting to the output capacitor, the proposed mechanism improves the stability of the single-phase energy conversion system. The experimental results verified the proposed method.

REFERENCES

[1] A. R. Gautam, K. Gourav, J. M. Guerrero, and D. M. Fulwani, "Ripple mitigation with improved line-load transients response in a two-stage DC–DC–AC converter: Adaptive SMC approach," *IEEE Trans. Ind. Electron.*, vol. 65, no. 4, pp. 3125–3135, Apr. 2018.

[2] D. Neumayr, G. C. Knabben, E. Varescon, D. Bortis, and J. W. Kolar, "Comparative evaluation of a full- and partial-power processing active power buffer for ultracompact single-phase DC/AC converter systems," *IEEE Trans. Emerg. Sel. Topics Power Electron.*, vol. 9, no. 2, pp. 1994–2013, Apr. 2021.

[3] S. Qin, Y. Lei, C. Barth, W.-C. Liu, and R. C. N. Pilawa-Podgurski, "A high power density series-stacked energy buffer for power pulsation decoupling in single-phase converters," *IEEE Trans. Power Electron.*, vol. 32, no. 6, pp. 4905–4924, Jun. 2017.

[4] H. Li, K. Zhang, H. Zhao, S. Fan, and J. Xiong, "Active power decoupling for high-power single-phase PWM rectifiers," *IEEE Trans. Power Electron.*, vol. 28, no. 3, pp. 1308–1319, Mar. 2013.

[5] Y. Tang, F. Blaabjerg, P. C. Loh, C. Jin, and P. Wang, "Decoupling of fluctuating power in single-phase systems through a symmetrical half-bridge circuit," *IEEE Trans. Power Electron.*, vol. 30, no. 4, pp. 1855–1865, Apr. 2015.

[6] S. Li, W. Qi, S.-C. Tan, and S. Y. Hui, "Integration of an active filter and a single-phase ac/dc converter with reduced capacitance requirement and component count," *IEEE Trans. Power Electron.*, vol. 31, no. 6, pp. 4121–4137, Jun. 2016.

[7] S. Qin, Y. Lei, C. Barth, W.-C. Liu, and R. C. N. Pilawa-Podgurski, "A high-efficiency high energy density buffer architecture for power pulsation decoupling in grid-interfaced converters," in *Proc. IEEE Energy Convers. Congr. Expo.*, 2015, pp. 149–157.

[8] W. Cai, B. Liu, S. Duan, and L. Jiang, "An active low-frequency ripple control method based on the virtual capacitor concept for BIPV systems," *IEEE Trans. Power Electron.*, vol. 29, no. 4, pp. 1733–1745, Apr. 2014.

[9] Y. Tang and F. Blaabjerg, "Power decoupling techniques for single-phase power electronics systems—An overview," in *Proc. IEEE Energy Convers. Congr. Expo.*, 2015, pp. 2541–2548.

[10] Y. Sun, Y. Liu, M. Su, W. Xiong, and J. Yang, "Review of active power decoupling topologies in single-phase systems," *IEEE Trans. Power Electron.*, vol. 31, no. 7, pp. 4778–4794, Jul. 2016.

[11] S. Li, G.-R. Zhu, S.-C. Tan, and S. Y. Hui, "Direct AC/DC rectifier with mitigated low-frequency ripple through inductor-current waveform control," *IEEE Trans. Power Electron.*, vol. 30, no. 8, pp. 4336–4348, Aug. 2015.

[12] Y. Tang, W. Yao, P. C. Loh, and F. Blaabjerg, "Highly reliable transformerless photovoltaic inverters with leakage current and pulsating power elimination," *IEEE Trans. Ind. Electron.*, vol. 63, no. 2, pp. 1016–1026, Feb. 2016.

[13] T. Shimizu, T. Fujita, G. Kimura, and J. Hirose, "A unity power factor PWM rectifier with DC ripple compensation," *IEEE Trans. Ind. Electron.*, vol. 44, no. 4, pp. 447–455, Aug. 1997.

[14] G.-R. Zhu, S.-C. Tan, Y. Chen, and C. K. Tse, "Mitigation of low-frequency current ripple in fuel-cell inverter systems through waveform control," *IEEE Trans. Power Electron.*, vol. 28, no. 2, pp. 779–792, Feb. 2013.

[15] R. Wang et al., "A high power density single-phase PWM rectifier with active ripple energy storage," *IEEE Trans. Power Electron.*, vol. 26, no. 5, pp. 1430–1443, May 2011.

[16] T. Shimizu, Y. Jin, and G. Kimura, "DC ripple current reduction on a single-phase PWM voltage-source rectifier," *IEEE Trans. Ind. Appl.*, vol. 36, no. 5, pp. 1419–1429, Sep./Oct. 2000.

[17] M. Su, P. Pan, X. Long, Y. Sun, and J. Yang, "An active power-decoupling method for single-phase AC–DC converters," *IEEE Trans. Ind. Inform.*, vol. 10, no. 1, pp. 461–468, Feb. 2014.

[18] Y. Tang, Z. Qin, F. Blaabjerg, and P. C. Loh, "A dual voltage control strategy for single-phase PWM converters with power decoupling function," *IEEE Trans. Power Electron.*, vol. 30, no. 12, pp. 7060–7071, Dec. 2015.

[19] Y. Tang and F. Blaabjerg, "A component-minimized single-phase active power decoupling circuit with reduced current stress to semiconductor switches," *IEEE Trans. Power Electron.*, vol. 30, no. 6, pp. 2905–2910, Jun. 2015.

[20] W. Yao, P. C. Loh, Y. Tang, X. Wang, X. Zhang, and F. Blaabjerg, "A robust DC-split-capacitor power decoupling scheme for single-phase converter," *IEEE Trans. Power Electron.*, vol. 32, no. 11, pp. 8419–8433, Nov. 2017.

[21] J. Zeng, M. Zhuo, H. Cheng, T. Kim, V. Winstead, and L. Wu, "Power pulsation decoupling for a two-stage single-phase photovoltaic inverter with film capacitor," in *Proc. IEEE Energy Convers. Congr. Expo.*, 2017, pp. 468–474.

[22] A. R. Gautam and D. Fulwani, "Second order harmonic ripple reduction in DC microgrid using sliding mode control approach," in *Proc. IEEE Int. Conf. Power Electron., Drives Energy Syst.*, 2016, pp. 1–6.

[23] S. Xu, L. Chang, R. Shao, and A. H. Mohomad, "Power decoupling method for single-phase buck-boost inverter with energy-based control," in *Proc. IEEE Appl. Power Electron. Conf. Expo.*, 2017, pp. 3426–3431.

[24] X. Chen, W. Wu, N. Gao, H. S.-H. Chung, M. Liserre, and F. Blaabjerg, "Finite control set model predictive control for LCL-filtered grid-tied inverter with minimum sensors," *IEEE Trans. Ind. Electron.*, vol. 67, no. 12, pp. 9980–9990, Dec. 2020.

[25] P. Falkowski and A. Sikorski, "Finite control set model predictive control for grid-connected AC–DC converters with LCL filter," *IEEE Trans. Ind. Electron.*, vol. 65, no. 4, pp. 2844–2852, Apr. 2018.

[26] T. Dragičević, "Model predictive control of power converters for robust and fast operation of AC microgrids," *IEEE Trans. Power Electron.*, vol. 33, no. 7, pp. 6304–6317, Jul. 2018.

[27] B. Liu, H. Wang, Y. Yang, X. Zhang, and B. Guo, "Improved model predictive control for single-phase grid-tied inverter with virtual vectors in the compacted solution-space," *IEEE Trans. Ind. Electron.*, vol. 69, no. 9, pp. 9673–9678, Sep. 2022.

[28] C. R. Baier, F. A. Villarroel, M. A. Torres, M. A. Pérez, J. C. Hernández, and E. E. Espinosa, "A predictive control scheme for a single-phase grid-supporting quasi-z-source inverter and its integration with a frequency support strategy," *IEEE Access*, vol. 11, pp. 5337–5351, 2023.

[29] R. O. Ramírez et al., "Finite-state model predictive control with integral action applied to a single-phase z-source inverter," *IEEE Trans. Emerg. Sel. Topics Power Electron.*, vol. 7, no. 1, pp. 228–239, Mar. 2019.

[30] S. Kwak, S.-E. Kim, and J.-C. Park, "Predictive current control methods with reduced current errors and ripples for single-phase voltage source inverters," *IEEE Trans. Ind. Inform.*, vol. 11, no. 5, pp. 1006–1016, Oct. 2015.

[31] Z. Qin, Y. Tang, P. C. Loh, and F. Blaabjerg, "Benchmark of AC and DC active power decoupling circuits for second-order harmonic mitigation in kilowatt-scale single-phase inverters," *IEEE Trans. Emerg. Sel. Topics Power Electron.*, vol. 4, no. 1, pp. 15–25, Mar. 2016.

[32] H. Li, Y. Sun, Y. Liu, S. Xie, and M. Su, "Coordinate transformation-based nonlinear power decoupling control for differential buck grid-tied inverter," *IEEE Trans. Ind. Electron.*, vol. 70, no. 12, pp. 12201–12210, Dec. 2023.

[33] R. Rajamony, S. Wang, R. Navaratne, and W. Ming, "Multi-objective design of single-phase differential buck inverters with active power decoupling," *IEEE Open J. Power Electron.*, vol. 3, pp. 105–114, 2022.

[34] J. Jiang, S. Pan, J. Gong, F. Liu, X. Zha, and Y. Zhuang, "A leakage current eliminated and power oscillation suppressed single-phase single-stage nonisolated photovoltaic grid-tied inverter and its improved control strategy," *IEEE Trans. Power Electron.*, vol. 36, no. 6, pp. 6738–6749, Jun. 2021.

[35] X. Xu, M. Su, Y. Sun, B. Guo, H. Wang, and G. Xu, "Four-switch single-phase common-ground PV inverter with active power decoupling," *IEEE Trans. Ind. Electron.*, vol. 69, no. 3, pp. 3223–3228, Mar. 2022.

[36] J. Hu, Q. Xu, P. Guo, J. Zhang, C. Tang, and A. Luo, "Ripple frequency independent power decoupling control method for single phase converter," *CPSS Trans. Power Electron. Appl.*, vol. 8, no. 3, pp. 234–245, Sep. 2023.

[37] R. A. Fantino, C. A. Busada, and J. A. Solsona, "Active power decoupling by closed-loop control of power oscillations for a bidirectional single-phase DC–AC converter," *IEEE Trans. Power Electron.*, vol. 38, no. 10, pp. 12446–12454, Oct. 2023.

[38] P. Nandi and R. Adda, "An active power decoupling-integrated reduced-switch current-fed switched inverter," *IEEE Trans. Emerg. Sel. Topics Power Electron.*, vol. 11, no. 2, pp. 1929–1942, Apr. 2023.

[39] A. R. Paul, A. Bhattacharya, and K. Chatterjee, "A novel single phase grid connected transformer-less solar micro-inverter topology with power decoupling capability," *IEEE Trans. Ind. Appl.*, vol. 59, no. 1, pp. 949–958, Jan./Feb. 2023.

[40] E. Heydari, A. Y. Varjani, and D. Diallo, "A dual-function power decoupling circuit for single-stage grid-connected PV inverter," *IEEE Trans. Power Electron.*, vol. 37, no. 6, pp. 7422–7431, Jun. 2022.

[41] I. Osman, D. Xiao, M. F. Rahman, M. Norambuena, and J. Rodriguez, "Discrete space vector modulation based model predictive flux control with reduced switching frequency for IM drive," *IEEE Trans. Energy Convers.*, vol. 36, no. 2, pp. 1357–1367, Jun. 2021.

[42] M. Gu et al., "Finite control set model predictive torque control with reduced computation burden for PMSM based on discrete space vector modulation," *IEEE Trans. Energy Convers.*, vol. 38, no. 1, pp. 703–712, Mar. 2023.

[43] S. Eren, M. Pahlevani, A. Bakhshai, and P. Jain, "An adaptive droop DC-bus voltage controller for a grid-connected voltage source inverter with LCL filter," *IEEE Trans. Power Electron.*, vol. 30, no. 2, pp. 547–560, Feb. 2015.